ISSN: 2688-9323

A New Type of MCT Device with Low Turn-off Loss

Xue Li

Southwest Jiao Tong University, Chengdu 611756, China

13668048432@163.com

Abstract

A novel MCT device for reducing the Turn-off loss of gated thyristor is proposed. In the novel MCT device, two P-type regions with different doping concentrations are introduced and an embedded NMOS structure is connected by floating electrodes. Two P-type regions with different doping concentrations separate the carriers to form two different channels. The floating electrode above the hole channel is connected to the upper end of the embedded NMOS structure through a wire to control the hole current. The MEDICI simulation results show that the Turn-off loss of the device is reduced by 39% under the same forward voltage drop.

Keywords

MOS Controlled Thyristor (MCT); Thyristor; Forward Voltage Drop (V_{on}); Turn-off Loss (E_{off}).

1. Introduction

For the gate-controlled thyristor (MCT), it has extremely low on-voltage drop and strong high current load capacity [1-3]. In recent years, MCT have attracted extensive attention in the field of power devices because of these excellent properties. However, for MCT, a negative bias voltage needs to be applied during Turn-off, the Turn-off process is complicated and the loss is large.

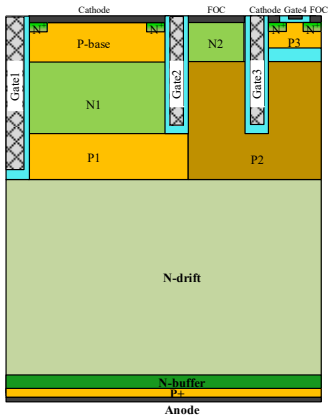

Fig 1. The schematic cross sections of proposed MCT

Aiming at this shortcoming of MCT , researchers have made a series of improvements. The anode short-circuit MCT (AS-MCT) designed in the literature [4-6], the bottom of the device is composed of alternating P+ doping and N+ doping from conventional P+ doping. Such a structural design makes the N+ doping at the bottom of the device short-circuited with the base of the PNP transistor. When turned off, the carriers present in the MCT can enter the anode directly through the N+ doped region at the bottom without passing through the P+ anode doped region. It enables faster Turn-off of the MCT. The cathode short-circuit type MCT (CS-

ISSN: 2688-9323

MCT) designed in the literature [7,8] increases the P+ type doping in the cathode region of the device, so that the cathode of the device is short-circuited with the base region of the NPN transistor to form a carrier channel. This region provides a channel for the extraction of hole carriers when Turn-off. At the same time, the gain of the NPN transistor is suppressed and the positive feedback inside the device is destroyed.

After some improvements, the Turn-off loss of the MCT device has been reduced, but in general, the Turn-off loss of the MCT is still relatively large and the speed is slow. To solve this problem, based on the conventional MCT structure, P1 and P2 regions with different doping concentrations and embedded NMOS structure are introduced in this paper to form a novel MCT . The novel MCT separates electron and hole carriers to form two channels for electron current and hole current. The top of the hole channel is connected to the embedded NMOS structure through a floating electrode, so as to control the holes. The MEDICI simulation results show that when the MCT is Turn-off, the speed of the novel MCT is significantly improved. When the forward voltage drop is both 1.2V, the Turn-off loss of the novel MCT is reduced from 1.73mJ to 1.05mJ, and it is reduced by 39%.

2. Structure and Mechanism

Fig. 1 shows the schematic cell units of proposed MCT. Two regions of P1 and P2 with different doping concentrations and an embedded NMOS structure are introduced. The excess carriers in the MCT are controlled by the two regions P1 and P2 and the embedded NMOS structure.

In the novel MCT, the doping concentration of the P2 region is higher. Hole carriers tend to flow into the high-concentration P2 region, while electron carriers tend to flow into the low-concentration P1 region. Therefore, the novel MCT can smoothly separate electron and hole carriers. On the left side of the MCT, the electron current channel is formed; on the right side of the MCT, the hole current channel is formed. When the MCT device is forward conducting stably, there are a lot of excess carriers in its drift region. During Turn-off, these excess carriers must be recombined or extracted, which leads to a long Turn-off time and a large Turn-off loss.

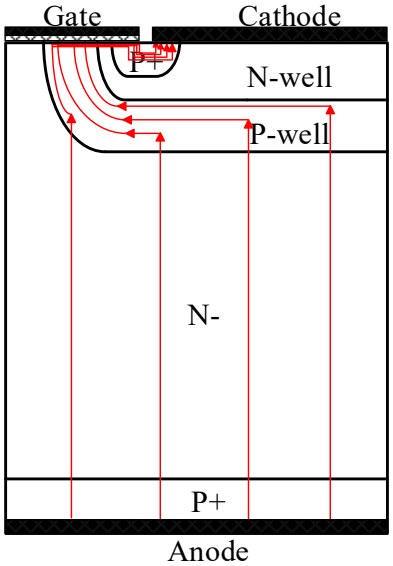

Fig 2. Current line distribution of the conventional MCT during Turn-off

For the conventional MCT, it mainly depends on PMOS structure when it is turne-off, and all the current flows away from this channel [9]. Fig. 2 shows the current line distribution when the MCT is turned off, and its equivalent circuit is shown in Fig. 3.It can be seen that when the gate voltage of the device changes from positive voltage to 0V or negative voltage. The NMOS responsible for turning on in the MCT is turned off, the base drive current inside the thyristor

ISSN: 2688-9323

disappears, and the positive feedback structure is destroyed. At the same time, the PMOS structure responsible for Turn-off is opened, providing a channel for excess carriers in the drift region to be pumped away, and preventing carrier regeneration inside the thyristor.

Since only one PMOS works in the conventional MCT device, the current tailing time of the device is long and the Turn-off loss is large. In response to this problem, in the novel MCT, the hole channel is connected to the NMOS structure through the floating electrode. So that the hole carriers in the device can be controlled by the electrodes. In this way, when the novel MCT is turned off, the excess carriers in the device are mainly controlled by the NMOS, and are quickly drawn away from the hole channel. Therefore, the novel MCT successfully shortens the Turn-off time and reduces the Turn-off loss.

The P1 and P2 regions in the device are similar to a PN junction structure, and their carrier distribution is also similar to that of the PN junction. Therefore, the P1 and P2 regions are directly regarded as a PN junction, and their carrier distribution is analyzed from the perspective of the PN junction. Since the P1 and P2 regions are both P-type doped, the analysis is mainly focused on the distribution of electrons.

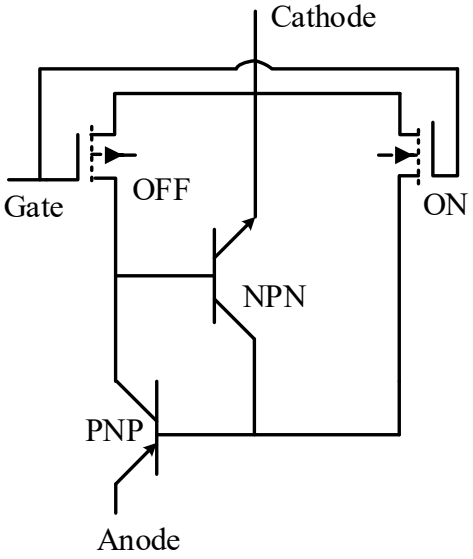

Fig 3. Equivalent circuit of conventional MCT

In the P1 region of the device, the distribution of electrons has the following expression [10]:

$$\frac{d^2 n_{p1}}{dx^2} = \frac{n_{p1}}{L_1^{\,2}} \tag{1}$$

Among them, the boundary conditions is:

$$\begin{aligned} n_{p1}(-x_p) &= n_{po1}\exp(\frac{eV}{KT}), x = -x_p \\ n_{P1}(x \to -\infty) &= n_{P01}, x \to -\infty \end{aligned} \tag{2}$$

Combining formula (1) and formula (2), the distribution of minority carriers in the P1 region is obtained:

$$n_{p1}(x) = n_{po1}\exp(\frac{eV}{KT})\exp(\frac{x + x_p}{L_1}) \tag{3}$$

ISSN: 2688-9323

Similarly, in the P2 region, the minority carrier distribution expression and boundary conditions are:

$$\frac{d^2 n_{p2}}{dx^2} = \frac{n_{p2}}{L_2^{\ 2}} \tag{4}$$

$$\begin{aligned} n_{p2}(x_n) &= n_{po2} \exp(\frac{eV}{KT}), x = x_n \\ n_{P2}(x \to \infty) &= n_{P02}, x \to \infty \end{aligned} \tag{5}$$

Combining formula (4) and formula (5), the distribution of minority carriers in the P2 region is obtained:

$$n_{p2}(x) = n_{po2} \exp(\frac{eV}{KT}) \exp(-\frac{x - x_n}{L_2}) \tag{6}$$

According to formula (3) and formula (6), we can know the ratio of minority carrier distribution between the two at any position x in the P1 and P2 regions:

$$\frac{n_{p1}(x)}{n_{p2}(x)} = \frac{N_{p2}}{N_{p1}} \exp(\frac{3x + x_p - 2x_n}{2L_2}) \tag{7}$$

$$\begin{aligned} x_n &= (\frac{2\varepsilon_s V_{bi}}{q} \times \frac{N_a}{N_d} \times \frac{1}{N_a + N_d})^{1/2} \\ x_p &= (\frac{2\varepsilon_s V_{bi}}{q} \times \frac{N_d}{N_a} \times \frac{1}{N_a + N_d})^{1/2} \end{aligned} \tag{8}$$

Substituting Equation (8) into Equation (7), and simplifying the ratio of minority carrier distribution in the P1 and P2 regions, we get:

$$\begin{aligned} \frac{n_{p1}(x)}{n_{p2}(x)} &= \frac{N_{p2}}{N_{p1}} \exp(\frac{3x + x_p - 2x_n}{2L_2}) \\ &= \frac{N_{p2}}{N_{p1}} \exp(\frac{3x + 37.5x_n - 2x_n}{2L_2}) \\ &= \frac{N_{p2}}{N_{p1}} \exp(\frac{3x + 35.5x_n}{2L_2}) \end{aligned} \tag{9}$$

because

$$L_2 = \sqrt{\mu_2 \frac{kT}{q} \tau} \tag{10}$$

Therefore, the ratio of minority carrier distribution in the two regions of P1 and P2 is obtained by final simplification:

ISSN: 2688-9323

$$\frac{n_{p1}(x)}{n_{p2}(x)} = \frac{N_{p2}}{N_{p1}} \exp(\frac{3x + 35.5x_n}{2L_2})$$
$$= 37.5 \exp(\frac{3x + 35.5x_n}{2L_2}) \quad (11)$$
$$>> 10$$

According to the above analysis result (11), it can be known that the concentration of minority carriers in the P1 region is more than 10 times than that in the P2 region, that is, the concentration of minority carriers in the P1 region is much higher than that in the P2 region. The electron concentration shows the purpose of separating electron and hole carriers is successfully achieved.

3. Simulation Results and Discussion

Table 1. Key design parameters of novel MCT

Parameters	Value	Unit
Width of cell	20	μm
Width of P-base	9	μm
Width of P1	10	μm
Width of P3	4	μm
Width of N2	4	μm
Depth of P-base	3	μm
Depth of N1	9	μm
Depth of P1	3	μm
Depth of P3	2	μm
Depth of N-drift	75	μm
Concentration of P-base	$1x10^{17}$	cm^{-3}
Concentration of P1	$2x10^{16}$	cm^{-3}
Concentration of P2	$3x10^{18}$	cm^{-3}
Concentration of P3	$8x10^{16}$	cm^{-3}
Concentration of N1	$5x10^{16}$	cm^{-3}
Concentration of N2	$3x10^{16}$	cm^{-3}
Concentration of N-drift	$1x10^{13}$	cm^{-3}
Concentration of buffer	$5x10^{17}$	cm^{-3}
Concentration of P+	$1.75x10^{18}$	cm^{-3}

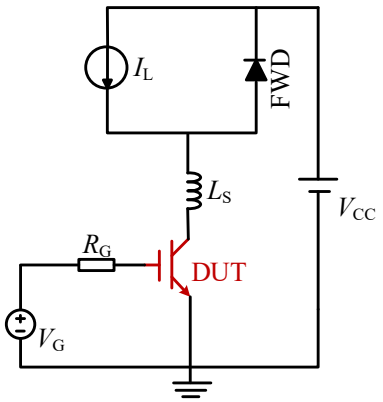

Fig 4. Simulation circuit of Turn-off characteristic

ISSN: 2688-9323

Two-dimensional simulation of MCT is verified by simulator MEDICI [11] and the physical models-*ANALYTIC* (carrier mobility model dependent on concentration and temperature), *FLDMOB* (carrier mobility model dependent on transverse field), *PRPMOB* (carrier mobility model dependent on perpendicular electric field), *CONSRH* (Shockley-Read-Hall recombination model dependent on concentration), *AUGER* (Auger recombination model), *BGN* (Slotboom bandgap narrowing model), and *IMPACT.I* (impact ionization model) are included. The key design parameters of novel MCT is given in Table I. Unless otherwise specified, some of the above parameters will be applied to other comparison structures.

Fig. 4 shows the simulation circuit of Turn-off. Among them, power supply voltage V_{CC}=600V; I_L=100A/cm^2; FWD is a freewheeling diode; inductance L_s=0.1nH; gate resistance R_G=10Ω; gate voltage V_G=15V. At Turn-off, the gate voltage drops from 15V to 0V and the device begins to turn off.

Fig. 5 shows the current line distribution inside the novel MCT at different times during the Turn-off process. It can be seen that at t=200μs, the device just begins to enter the off state. At this time, there is still electron injection in the device, and current lines flow in the P1 and P2 regions. With the passage of time, when t=201.62μs, all the current lines pass through the P2 region and then enter the NMOS structure, indicating that the excess carriers in the device are controlled by the embedded NMOS structure. The existence of this structure provides a channel for the extraction of excess carriers.

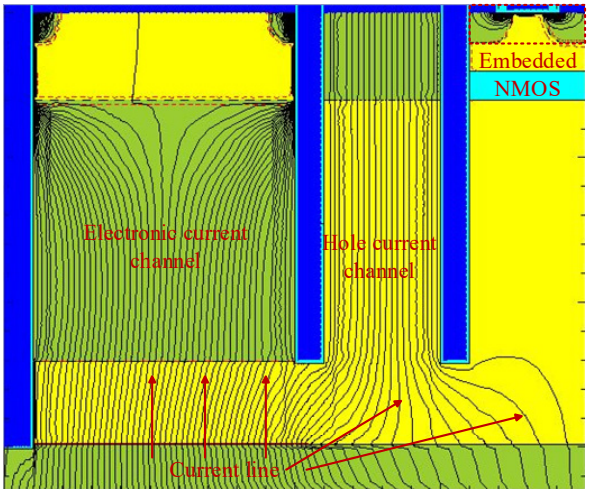

(a) t=200μs

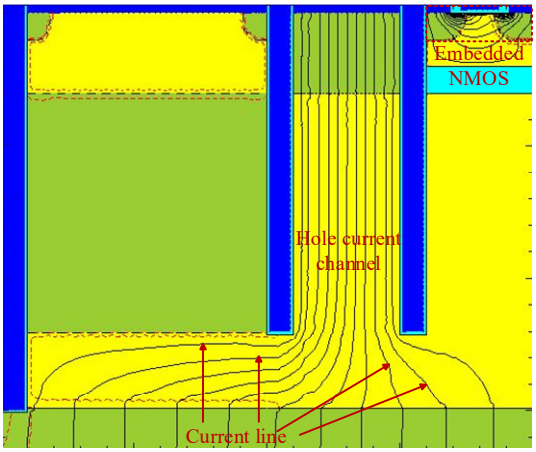

(b) t=201.62μs

Fig 5. Current line distribution when the novel MCT is turned off

ISSN: 2688-9323

Fig. 6 shows the current line distribution when the conventional MCT is turned off. It can be seen that the conventional MCT only one channel during turn-on or Turn-off, and the excess carriers in the device are not controlled in any way. Therefore, the Turn-off speed of conventional MCT is significantly slower and the losses are correspondingly larger compared to the novel MCT devices.

Figs. 7 shows the comparison of the Turn-off curves of the novel MCT and the conventional MCT. It can be seen that compared with the conventional MCT, the tail current of the new MCT is significantly smaller. The integral between 10% of the maximum anode voltage of the device (600V) and 10% of the maximum anode current (100A/cm^2) is the Turn-off loss. When the forward voltage drops of the devices are all 1.2V, the Turn-off loss of the conventional MCT is E_{off}=1.73mJ.

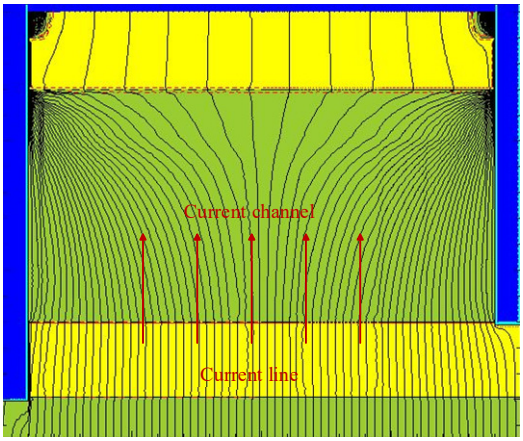

(a) t=200μs

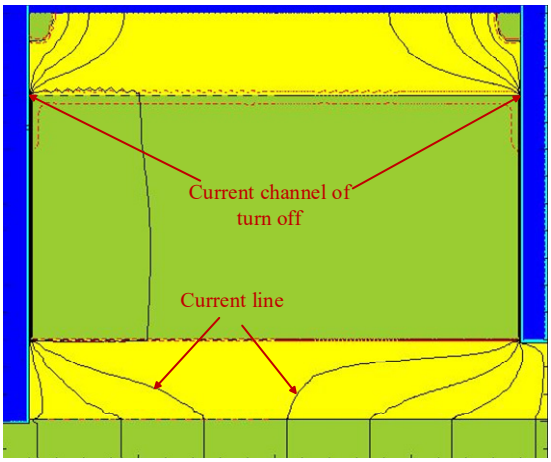

(b) t=202.05μs

Fig 6. Current line distribution when the conventional MCT is turned off

while the novel MCT is E_{off}=1.05mJ. The Turn-off loss of the novel MCT device is 24% lower than that of the conventional MCT, which shows that the novel MCT has a reasonable structure design, and can successfully extract the excess carriers in the drift region quickly to achieve the purpose of reducing the Turn-off loss.

ISSN: 2688-9323

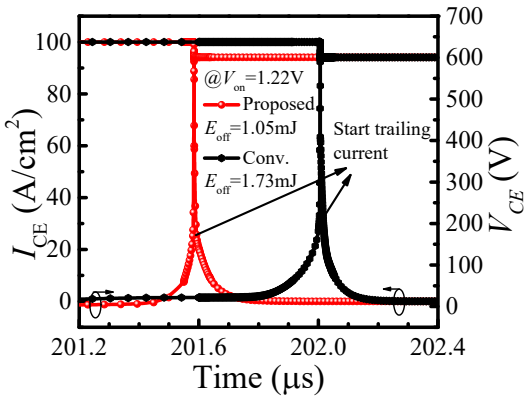

Fig 7. Turn-off curves of novel MCT and comparative structures

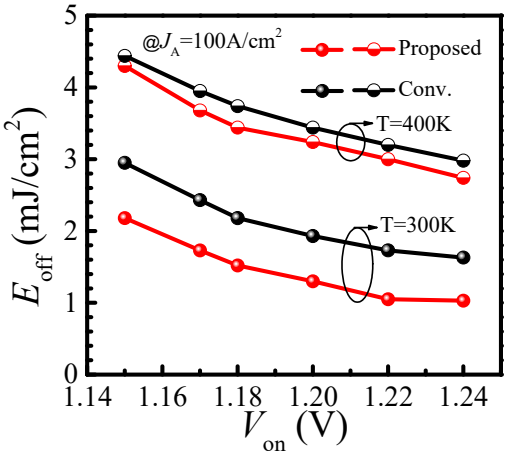

Fig 8. V_{on}-E_{off}

Fig. 8 shows the trade-off between forward voltage drop (V_{on}) and Turn-off loss (E_{off}) for novel MCT and conventional MCT. It can be seen that no matter T=300K or T=400K, the Turn-off loss of the novel MCT is smaller than that of the conventional MCT under any of the same forward voltage drop values. It can be seen that the novel MCT device designed in this paper has a better trade-off relationship between the forward voltage drop and the Turn-off loss, and has better comprehensive performance.

4. Conclusion

In this paper, a novel MCT is proposed based on the conventional MCT structure. It can provide a channel for the extraction of excess carriers in the device, solve the problems of long tail current time and large Turn-off loss of conventional MCT, and improve the trade-off relationship between forward voltage drop and Turn-off loss.

References

[1] Temple V A K. MOS controlled thyristors (MCT's) [C]. IEEE International Electron Devices Meeting, 1984:282-285.

[2] Baliga B. Fundamentals of Power Semiconductor Devices [M]. America: Springer, 2008, 653-654.

[3] Blicher A. Thyristor physics [M]. 1976.

ISSN: 2688-9323

[4] Chernyavsky E V, Popov V P, Krasnikov Y S, et al. Carrier lifetime and Turn-off current control by electron irradiation of MCT [J]. Nuclear Inst & Methods in Physics Research B, 2002, 186(1-4):157-160.

[5] Li L, Li Z H, Ren M, et al. Experimental Study on Displacement Damage Effects of Anode-Short MOS-Controlled Thyristor [J]. IEEE Transactions on Nuclear Science, 2020, 67:508-517.

[6] Li L, Li Z H, Chen X C, et al. A Study on Ionization Damage Effects of Anode-Short MOS-Controlled Thyristor [J]. IEEE Transactions on Nuclear Science, 2020, 67:2062-2072.

[7] Chen W, Liu C, Tang X, et al. Experimentally demonstrate a cathode short MOS-controlled Thyristor (CS-MCT) for single or repetitive pulse applications [C]. 28th International Symposium on Power Semiconductor Devices and ICs (ISPSD), IEEE, 2016.

[8] Yang Y X, Chen W J, Zhang H Y, et al. Evaluation of an Effective DC Solid State Circuit Breaker Based on CS-MCT [C]. IEEE Electron Devices Technology and Manufacturing Conference, 2021.

[9] Jahns T M, De Doncker R W A A, Wilson J W A, et al. Circuit utilization characteristics of MOS-controlled thyristors [J]. IEEE Transactions on Industry Applications, 1991, 27(3):589-597.

[10] DA Neamen. Semiconductor Physics and Devices [J]. materials today, 2012.

[11] Medici User Guide, Version D-2010.03, Synopsys Inc, Mountain View, CA, USA, 2010.